Novel Chemical Methods for the Infiltration of Opal Particles with Electrically Conductive Polyaniline Polymers

Hanaa S. A. Khalil,[1]* Kalle Levon[2]

[1]*Department of Energy Sciences and Technology, Brookhaven National Laboratory, Upton, New York 11973*
[2]*Department of Materials Chemistry, Polytechnic University, Brooklyn, New York 11201*

Received 3 August 2001; accepted 1 April 2002

ABSTRACT: Chemical methods for successfully coating opal particles with electrically conducting polyaniline (PANi) polymers were studied. Two different routes were proven successful. First was the *in situ* chemical doping reaction of PANi with dodecylbenzenesulfonic acid (DBSA) and camphorsulfonic acid dopants. The other method was placement of opal particles in a low concentration of a conducting PANi/DBSA solution in chloroform. Ultraviolet analyses of opal samples showed typical spectra for doped PANi with delocalized polarons. The electrical resistance of coated opal was measured to be 0.75×10^3 Ω. Morphological studies of the fractured surface by scanning electron microscopy indicated successful coating. Cyclic voltammetry studies confirmed the percolating behavior of infiltrated PANi. Also, a selective electroactive behavior toward the type of dopant was observed. © 2002 Wiley Periodicals, Inc. J Appl Polym Sci 86: 788–793, 2002

Key words: opal; photonic; polyaniline; infiltration

INTRODUCTION

Synthetic opal particles are three-dimensional periodic structures formed from nanoparticles of silica suspended in solutions.[1–3] The slow sedimentation of the silica particles onto a pattern substrate can direct the sedimented particles into an ordered pattern to yield photonic crystals. These have several potential applications in the field of optoelectronics and important technological uses as optical switches, optical filters,[4–7] and materials with photonic band gaps (PBGs).[8,9]

The period of the three-dimensional structure of opal is close to the wavelength of electromagnetic (EM) waves.[10] In such photonic crystals, the EM radiation undergoes Bragg's diffraction, forming a stop band for all modes propagating in a given direction.[11–13] The absence of the propagating EM radiation inside PBGs gives rise to unusual quantum phenomena, such as the inhibition of spontaneous emission.[14] The difference between the refractive index of the silica spheres and that of the surrounding media are responsible for the PBG, pseudogap, or a complete optical homogeneity where the PBG completely disappears.

Opals are insulating materials with resistivities of more than 10^{11} Ω/cm. That inhibits the use of this unique material in many applications that require a minimum value of electrical conductivity.

A few different methods have been tried recently to infiltrate opal with semiconducting metals, alloys[15–17] and conducting polymers.[18–20] One possible way to enhance the properties would be control of refractive indices by an electric field.

In this study, the infiltration of opal particles with electroconductive polyaniline (PANi) via *in situ* chemical doping reaction was examined. Our goal was to achieve a material with a special value of conductivity or possibility to control the optical properties of opal as a photonic crystal The evidence of the successful coating of opal and of filling the gaps between its spheres were studied. Optical, morphological, and electrical properties and the electrochemical behavior of this material were monitored.

EXPERIMENTAL

Opal samples were supplied by Allied Signal Co. (Morristown, NJ). Aniline, dodecylbenzenesulfonic acid (DBSA), camphorsulfonic acid (CSA), and chloroform were all Aldrich (St. Louis, MO) products and were used as supplied.

In situ doping of PANi

Small rectangular samples of 0.5 mm thick opal were placed in a 100-mL round-bottomed flask. The doping reaction of PANi with DBSA was conducted in the presence of the opal particles. The details of the doping reaction was reported elsewhere.[21] The PANi:

Correspondence to: H. S. A. Khalil.
**Permanent address:* Department of Polymer Science, National Research Center, Cairo, Egypt.

Journal of Applied Polymer Science, Vol. 86, 788–793 (2002)

DBSA molar ratio was maintained at 1:0.5 with 1 g of PANi and 4 g of DBSA. We allowed the doping reaction to occur by thermal heating at 90°C without any solvent. After the completion of the reaction, samples were washed with chloroform and allowed to dry. Another experiment was done with CSA as a dopant. The reaction was conducted as reported before with *m*-cresol as a solvent.[22] The opal sample was placed in a 500-mL flask. CSA (1.07 g) was allowed to dissolve in 100 g of *m*-cresol, and 1.04 g of PANi was added; the mixture was stirred for 48 h. The opal sample was taken and washed many times with chloroform.

Placement of opal particles in a dilute solution of conducting PANi/DBSA

A 4.0% (w/w) solution of PANi /DBSA in chloroform was prepared. Small samples of opal were placed in the solution for 24 h and were then washed with chloroform and dried in a vacuum oven.

Characterization

Ultraviolet (UV) analysis

We used an ultraviolet–visible (UV–vis) spectrometer (DMS-100, Varian Co.) to study the absorption spectra of infiltrated opal with PANi. An opal sample was placed in one sample holder and filled with chloroform, and the other one was filled with chloroform as a reference. Opal is transparent and allows the passage of light through it in chloroform. Samples were scanned from 200 to 900 nm with a scan rate 10 nm/s.

Scanning electron microscopy (SEM)

Morphological studies of infiltrated samples were performed with SEM. Samples were surface-fractured, coated with a thin layer of gold by evaporation, and studied by SEM.

Cyclic voltammetry (CV)

Opal samples infiltrated via *in situ* doping were coated with gold from one side and placed in one compartment of the microelectrochemical cell with a few drops of a 1*M* solution of H_2SO_4. CV was performed at a 50 mV/s sweep rate over the potential range −1 to 1 V versus a silver/silver chloride reference electrode. HCl (0.1*M*) was also used for CV measurements of opal infiltrated with PANi/CSA via *in situ* doping. Opal infiltrated with PANi/DBSA and with PANi/CSA was used as the working electrode.

Electrical conductivity measurements

The two-probe-point method was used for resistance measurements as a primary estimation of opal conductivity.

RESULTS AND DISCUSSION

The opal sample infiltrated with PANi/DBSA via the *in situ* doping reaction turned dark green with dark red and green reflections when placed in chloroform. The same color reflections were observed for fractured surfaces. Opal samples that were placed in different concentrations of PANi/DBSA solutions in chloroform turned different colors, from pale green to dark green.

The optical properties of opal particles infiltrated with PANi were studied by UV–vis spectroscopy. The UV spectrum of the pure opal particles supplied by Allied Signal is shown in Figure 1. A thin film of opal particles was cut from the bulk sample at an angle of 60°. A sharp peak was observed at 440 nm, and a small hump was observed between 560 and 650 nm. Also, a strong peak at a shorter wavelength was observed at 220–300 nm. The sharp peak at 440 nm has been assigned to a PBG or pseudogap,[23] whereas the strong peak at 220–300 nm may have originated from partial leakage of light from the detected beam due to scattering. The hump at the longer wavelength region at 560–650 nm may have been due to Raleigh-power-like dependence, reflecting an increase of the scattering cross-section.[24]

The spectral analysis of opal coated with PANi is shown in Figure 2. When the spectrum of pure opal (Fig. 1) is compared to opal infiltrated with PANi/DBSA via the *in situ* doping reaction (Fig. 2), it is seen that opal was extensively infiltrated with PANi/DBSA with delocalized polarons. The spectrum is basically typical of doped PANi. A peak at 440 nm was observed that was due to the polaron band to π^*-band transition in doped PANi. A broad hump was observed between 540 and 1100 nm, which was attributed to the π-band to polaron band transition in doped PANi, and this indicated delocalization of PANi/DBSA inside the opal particles.

The UV spectrum of opal infiltrated with PANi/DBSA via placement in a low concentration of PANi/DBSA is shown in Figure 3. The typical spectra of PANi/DBSA was observed with delocalized polarons. Two absorption peaks were observed at 464 nm and at 540 to 1100 nm. The extended broad band from 600 to 1100 nm indicated effective delocalized polarons of PANi inside the opal particles.

Both methods of infiltration showed similar UV spectra, which might have been generally due to the strong influence of opal silica particles on PANi.

Morphological studies of opal particles were achieved with SEM. Pictures of opal infiltrated with PANi via the *in situ* doping reaction are shown in Figures 4–6. Small spheres of opal were extensively coated with PANi/DBSA. The penetration of polymer was observed on the fractured surface of opal. The obvious hexagonal morphology of opal spheres, as

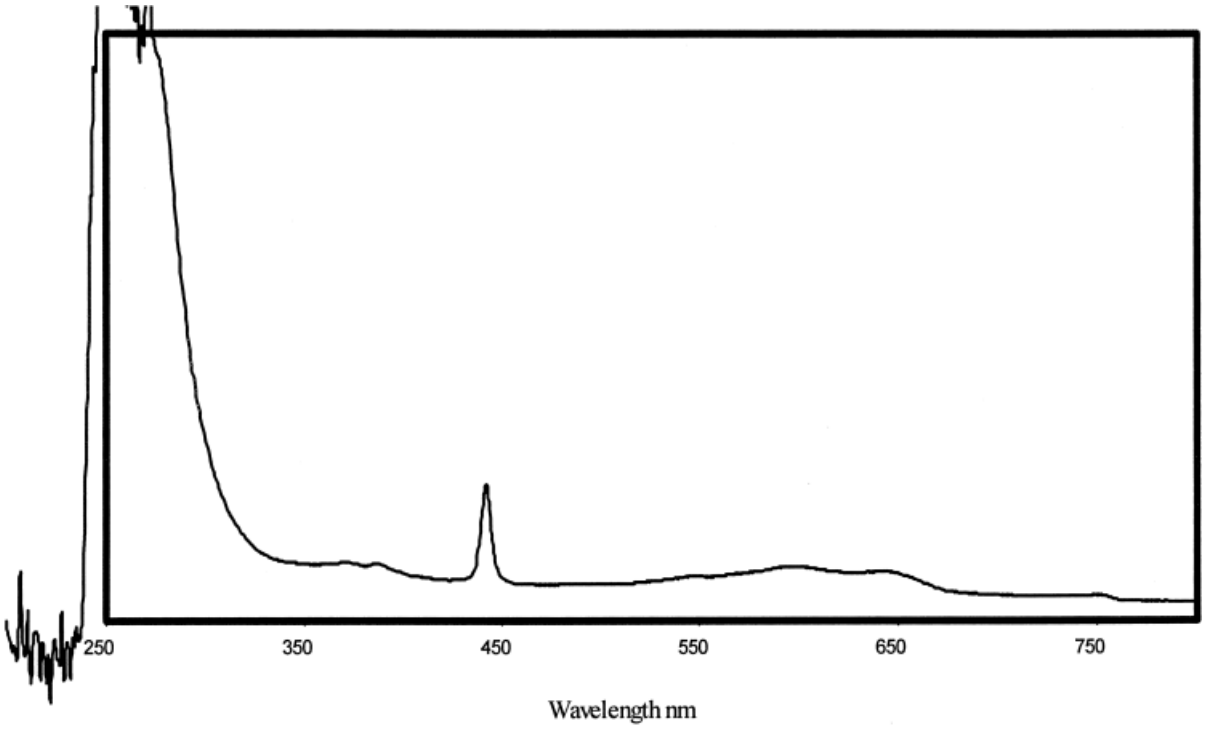

Figure 1 UV spectrum of opal particles.

shown in Figure 6, has been explained by the cleavage of the 111-plane.[25] The structure is mainly controlled by the geometry of the cavities. Homogeneous coating was observed. We concluded that PANi filled all channels and voids inside opal, which covered the entire close packing of opal as a continuous framework with inclusions of periodically spaced silica spheres. We also concluded that PANi inside silica particles had a continuous path, coated silica spheres, and filled out all voids among spheres.

Samples infiltrated via placement in solution indicated a resistance value of about 0.5×10^5 Ω with DBSA as a dopant. The opal itself had a resistance of about 10^{11}–10^{12} MΩ. With the *in situ* doping reaction,

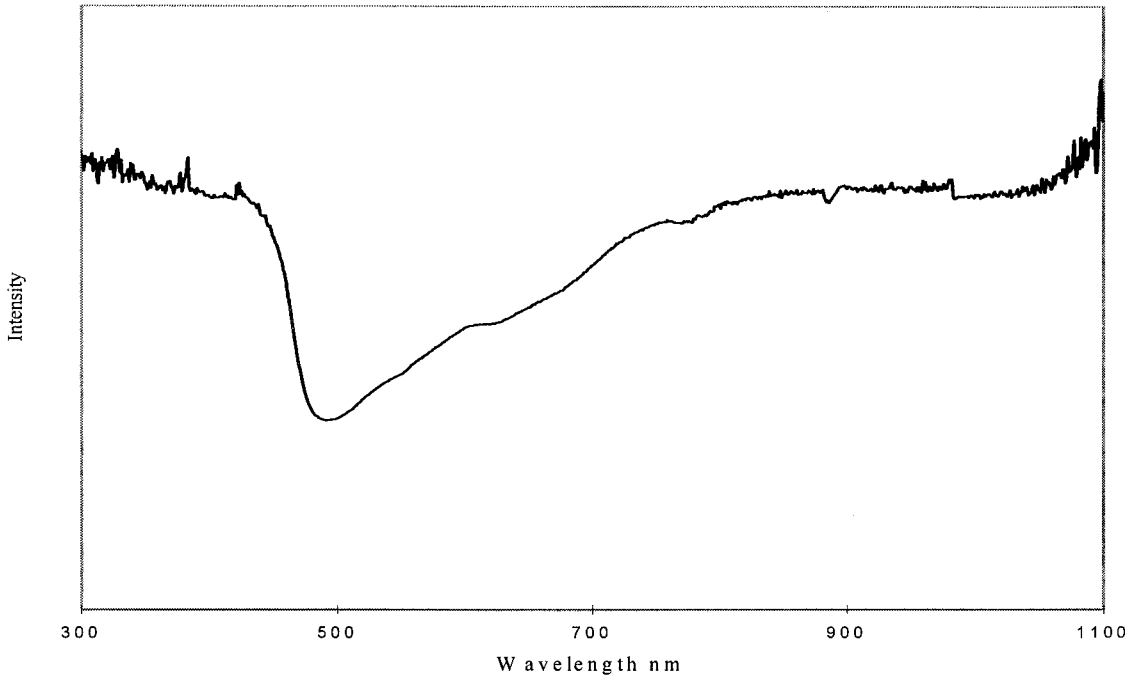

Figure 2 UV spectrum of opal particles infiltrated with PANi/DBSA via *in situ* doping.

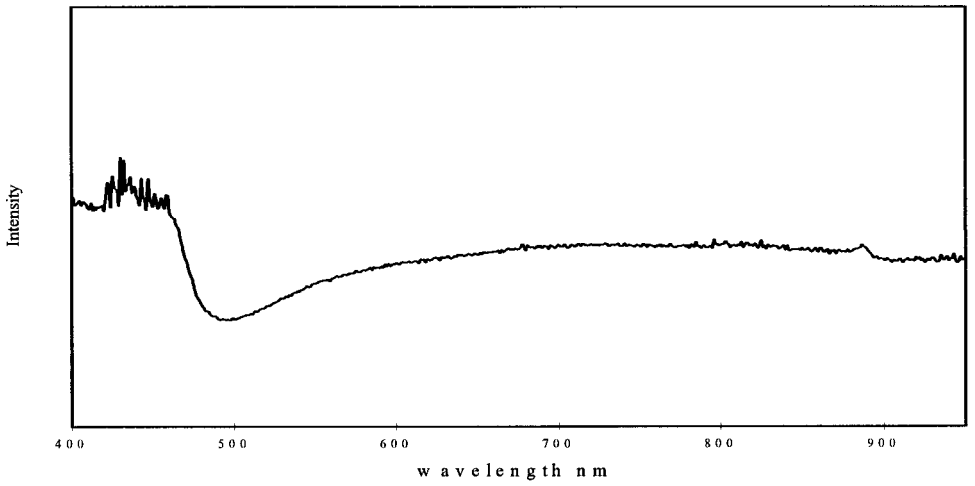

Figure 3 UV spectrum of opal particles infiltrated via placement in 4.5 wt % PANi/DBSA.

the resistance decreased to 1.7×10^3 Ω, a value comparable to that of ITO conductive glass. With CSA as a dopant, the resistance decreased more to 0.85×10^2 Ω. The electrical conductivity of opal was enhanced more than six orders of magnitude relative to the opal particle itself. This agreed with the observed UV–vis spectra of the delocalized polarons of doped PANi inside opal particles.

A cyclic voltammogram of opal particles infiltrated with PANi/DBSA via *in situ* doping is shown in Figure 7. Two distinctive peaks were observed for anodic polarization, and almost no peaks were observed in the cathodic current. The first peak was observed at −0.13 V and at −0.38 V. With PANi/CSA, two peaks were observed at the cathodic polarization, and no peaks were observed at the anodic current. A very long tail was observed at −1 and 1 V, respectively. The opal was cycled hundreds of times without showing any degradation of the polymer. It is well known that PANi has two oxidation peaks and two reduction peaks when in the protonated state. The electroactive behavior of PANi can be monitored by CV. During the electrochemical oxidation–reduction reaction of PANi, positive charges are created and destroyed in the polymer matrix. To maintain electroneutrality, ions have to be exchanged with the electrolyte solution.[24] Previous studies have shown that anions and protons are exchanged in aqueous solutions.[25] The first oxidation peak in the cyclic voltammogram of PANi in the positive current was due to the creation of positive charges via the oxidation of PANi, which could be explained by the following reaction:

$$(C_6H_4NH—)_2 \rightarrow \{(C_6H_4NH^-)^{\bullet+}\}\ 2 + 2e$$

Anions from solutions are inserted into the film, mainly chloride ions when hydrochloric acid is used

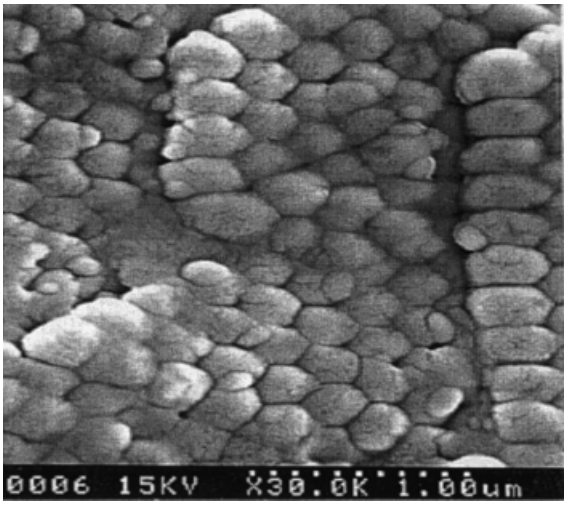

Figure 4 SEM of the fractured surface of opal particles infiltrated with PANi/DBSA via *in situ* doping.

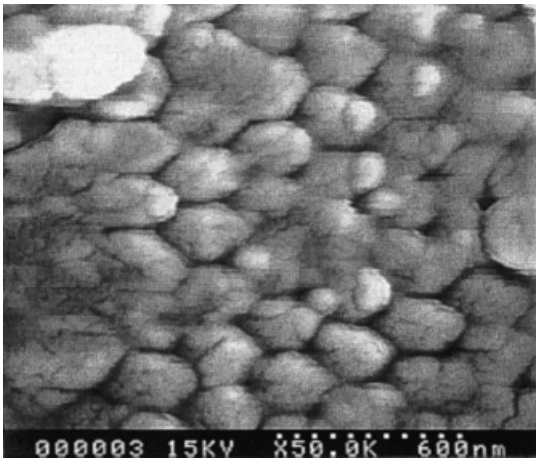

Figure 5 SEM of the fractured surface of opal particles coated with PANi/DBSA via *in situ* doping.

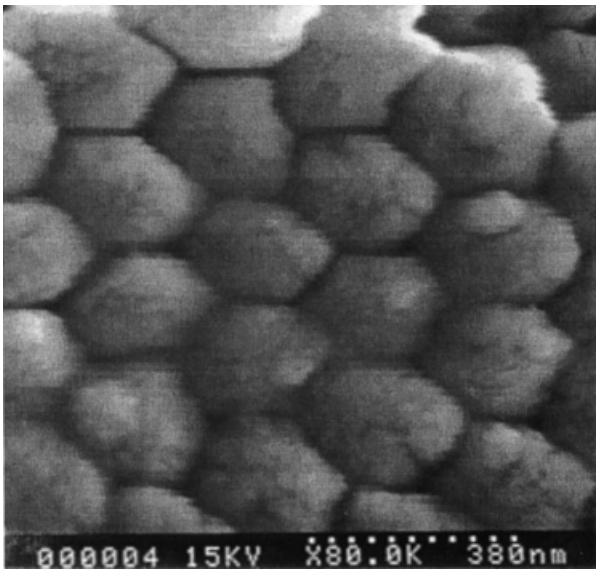

Figure 6 SEM of the hexagonal packing of opal particles infiltrated with PANi/DBSA.

to compensate for the positive charge formed. This causes the formation of emeraldine salt, the most conductive state in PANi. The second oxidation peak in the positive current in CV corresponded to the deprotonation of the imine nitrogen, which renders an uncharged matrix with expulsion of protons and anions; a state of pernigraniline oxidation forms the reaction mechanism, which could be represented as follows:

$$(C_6H_4NH—)_2^{+\cdot}(X)— \rightarrow (C_6H_4—N{=}C_6H_4{=}N)—$$

All reaction steps are supposed to be reversible by application of negative current if pernigraniline starts to be protonated.

In the infiltration of opal with PANi/DBSA, CV of PANi indicated clear distinctive peaks for oxidation, whereas the reduction peaks were almost obscured or too broad. This could be explained by the fact that the two electrochemical processes are different. During oxidation, the layer next to the electrode first becomes conducting and forms the electrode surface for the next layer and so on until the conducting zone reaches the solution interface. In reduction, however, the layer next to the electrode becomes nonconducting, and hence, the conduction path is interrupted. This slows down the kinetics, resulting in a broader CV peak.[24]

The opposite was observed in the case of opal infiltrated with PANi/CSA, where the oxidation peaks completely disappeared and two distinctive reduction peaks were observed in the cathodic current (Fig. 8). The opal had a selective reaction or response toward the electrochemical processes taking place inside its particles. We concluded that the oxidation–reduction reaction is not the same as it is in bulk PANi. In the case of PANi/CSA, the polymer underwent changes from the oxidized state to the reduced state without passing through the two-step oxidation–reduction reactions. The role of the opal toward the electroactive behavior of the polymer was not clear, and further studies are needed.

CONCLUSIONS

We successfully infiltrated opal particles with an emeraldine salt of PANi. *In situ* doping and placement in different concentrations were successful methods of achieving infiltration. *In situ* doping introduced a three-dimensional replica of a continuous path of conducting polymer inside opal particles. This was indicated by the high conductivity of opal and by morphological studies performed with SEM. CV of opal indicated elecroactive behavior of PANi with con-

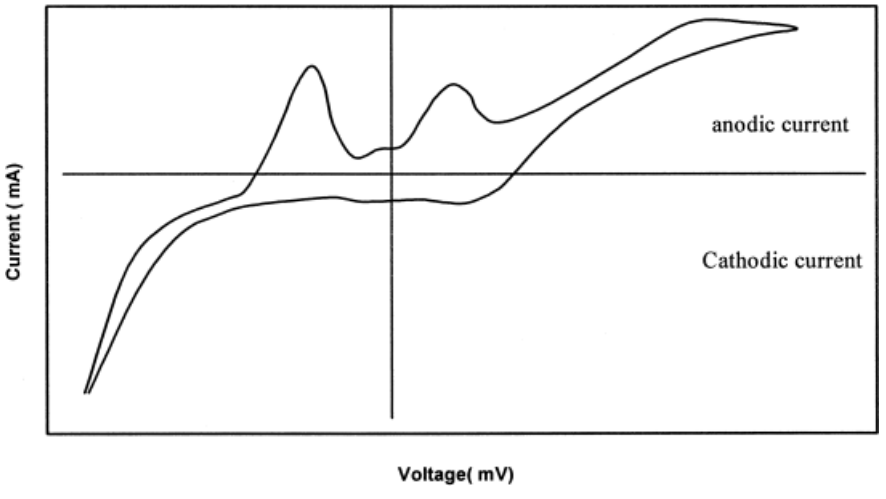

Figure 7 CV of opal particles infiltrated with PANi/DBSA.

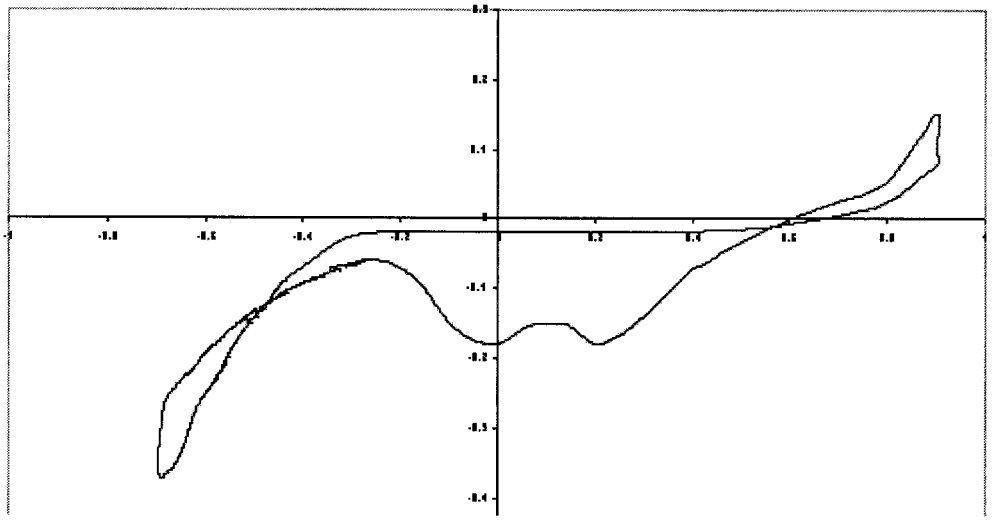

Figure 8 CV of opal particles infiltrated with PANi/CSA.

trolled oxidation–reduction steps that differed from that of bulk polymer. The advantage of the infiltration of opal particles could be used to create durable polymer that does not undergo an overoxidation reaction, which generally occurs in electroactive polymers. Both methods of infiltration of PANi in opal were proven to be successful.

References

1. Blaadern, A. V.; Ruel, R.; Wiltzius, P. Nature 1997, 385, 321.
2. Sacks, M. D.; Tseng, T. Y. J Am Ceram Soc 1984, 67, 525.
3. Johnson, N. P.; McComb, D. W.; Richel, A.; Treble, B. M.; De La Rue, R. M. Synth Met 2001, 116, 469.
4. Flaugh, P. L.; O'Donnell, S. E.; Asher, S. A. Appl Spectrosc 1984, 38, 847.
5. Kamenetzky, E. A.; Mangliocco, L. G.; Panzer, H. P. Science 1994, 263, 207.
6. Sunkara, H. B.; Jethmalani, J. M.; Ford, W. T. Chem Mater 1994, 6, 362.
7. López, C.; Blanco, A.; Míguez, H.; Meseguer, F. Opt Mater 1999, 13, 187.
8. Vos, W. L. Phys Rev B 1996, 53, 16231.
9. Tarhan, I. I.; Watson, G. H. Phys Rev Lett 1996, 76, 315.
10. Soukoulis, C. M. Photonic Band Gaps & Localization; NATO Advanced Study Institute, Series B: Physics; Plenum: New York, 1993.
11. Sözuer, H. S. Phys Rev B 1992, 45, 13962.
12. Sözuer, H. S. J Opt Soc Am B 1993, 10, 296.
13. Ho, K. M. Phys Rev Lett 1990, 65, 3152.
14. Yablonovitch, E. Phys Rev Lett 1987, 58, 2059.
15. Bogomolov, V. N. Ukr Fiz Zh 1987, 24, 171.
16. Eradat, N.; Haung, J. D.; Vardeny, Z. V.; Zakhidov, A. A.; Khayrullin, I.; Udod, I.; Baughman, R. H. Synth Met 2001, 116, 501.
17. Alekseev, A. Y.; Bogomolov, T. B.; Zhukova, I. Akad Nauk SSSR, Ser Fiz 1986, 50, 418.
18. Bogomolov, V. N.; Kumzerov, Y. A. Preprint No. 971; Fiz.-Tekh. Inst.: Leningrad, 1985.
19. (a) Bogomolov, V. N. Pis'ma Zh Eksp Teor Fiz 1982, 36, 298; (b) Bogomolov, V. N. JETP Lett 1982, 36, 365.
20. Eradat, N.; Wohlgenannt, M.; Vardeny, Z. V.; Zakhidov, A. A.; Baughman, R. H. Synth Met 2001, 116, 509.
21. Yoshino, K.; Kawagishi, Y.; Tatsuhara, S.; Kajii, H.; Lee, S.; Fujii, A.; Ozaki, M.; Zakhidov, A. A. Microelectron Eng 1999, 47, 49.
22. Levon, K.; Ho, K. H.; Zheng, W. Y.; Laakso, J.; Kärnä, T.; Taka, T.; Österholm, J. E. Polymer 1995, 36, 2731.
23. Cao, Y.; Smith, P.; Heeger, A. J. J. Synth Met 1992, 48, 91.
24. Aoki, K. J Electroanal Chem 1994, 373, 67.
25. Vlasov, Y. A.; Kaplyanskii, A. A. Phys Rev B 1997, 375, 55.